RSC Advances

This is an *Accepted Manuscript*, which has been through the Royal Society of Chemistry peer review process and has been accepted for publication.

Accepted Manuscripts are published online shortly after acceptance, before technical editing, formatting and proof reading. Using this free service, authors can make their results available to the community, in citable form, before we publish the edited article. This *Accepted Manuscript* will be replaced by the edited, formatted and paginated article as soon as this is available.

You can find more information about *Accepted Manuscripts* in the Information for Authors.

Please note that technical editing may introduce minor changes to the text and/or graphics, which may alter content. The journal's standard Terms & Conditions and the Ethical guidelines still apply. In no event shall the Royal Society of Chemistry be held responsible for any errors or omissions in this *Accepted Manuscript* or any consequences arising from the use of any information it contains.

ROYAL SOCIETY OF CHEMISTRY

www.rsc.org/advances

ARTICLE TYPE www. rsc.org/xxxxxx | XXXXXXXX

Optical enhancement of plasmonic activity of catalytic metal nanoparticles

Tomasz J. Antosiewicz[*ab] **and S. Peter Apell**[b]

Received Xth XXXXXXXXXX 20XX, Accepted Xth XXXXXXXXX 20XX
First published on the web Xth XXXXXXXXXX 200X
DOI: 10.1039/b000000x

Noble metals have recently been shown to drive direct photocatalytic reactions in which they both provide hot electrons via the localized surface plasmon resonance (LSPR) and the catalytically active site. Catalytic reactions are also possible on other metals such as platinum or rhodium which, however, exhibit rather poor plasmonic properties (low field enhancements, low resonance quality factors) and their LSPR for nanometer sized particles occurs in the UV, an unfavourable effect when considering sunlight as a photon source. By coupling the LSPR response of catalytic metal nanoparticles to that of a silver nanoparticle we can excite a hybridized resonance that matches the spectral characteristic of the light source and light absorption in the catalytic metal is enhanced by up to one order of magnitude. This is shown for a number of catalytic metals and is further discussed for model materials described by Drude and Drude-Lorentz dispersion. These results provide guidelines for designing catalytic metal nanostructures which absorb the solar spectrum very efficiently.

Introduction

Brought on by sophisticated experimental methods and theoretical tools, nanometer sized metal structures have been working their way into an increasing number of research fields such as photo-detection,[1] sensing,[2,3] cancer therapy,[4] waveguides,[5,6] and solar cells[7] – fields in which interaction of light with nanoparticles via localized surface plasmon resonances (LSPRs) is of key interest. Metals are likewise known for their role as catalysts and recent work demonstrated a promising route of utilizing LSPRs to drive/enhance photocatalytic reactions.[8–10]

An LSPR involved in a photocatalytic process may contribute to it indirectly – by transferring energy from the excited resonance to materials in the vicinity of the metal nanoparticle[11] – or via a direct process in which metal nanoparticles serve both as the plasmonic resonator and the catalytic material.[12] The efficiency of plasmon induced catalysis is limited by various factors, however, the one considered here is related to the electromagnetic interaction between light and the metal resonator. The transfer of energy can occur either radiatively, by scattering of enhanced electromagnetic fields, or nonradiatively, a process in which energetic electrons are generated.[13] These two processes, in principle, compete against each other and depending on the requirements, it is usually beneficial to maximize the desired channel. Yet, despite this trade-off, in any plasmon-assisted process it is of paramount importance to excite the plasmon as efficiently as possible.

In this work we analyse the plasmonic properties of heterometallic structures (nanoparticles) involved in direct photocatalysis: specifically, the focus is placed on poor plasmonic metals. These, in contrast to good metals (*e.g.* Au or Ag), have high losses in the visible and consequently low resonance quality factors and offer low field enhancements. The reason for choosing early transition metals rather than coinage ones is that, in general, noble metals are not the best catalytic metals[14] (for simplicity, when mentioning transition metals we address those except for Au and Ag). That being said, due to their low losses noble metals offer very large field enhancements and as a result are ideal model materials to study direct plasmon-assisted photocatalysis, as recent review articles illustrate.[13,15,16] Transition metals, however, which usually exhibit a poor plasmonic response, are known to catalyse many reactions[17,18] and could benefit from plasmon-assisted photocatalysis. The LSPR for a given size of a particle made from a transition metal is usually blueshifted in comparison to silver or gold. Placing them on a substrate will redshift the response, however, catalytic metal nanoparticles have, in general, their LSPR in the UV. Thus, one major disadvantage of plasmon-assisted photocatalysis on transition metals is a lack of spectral overlap between the solar spectrum (for sunlight energy harvesting) and the plasmonic response of such metals. Hence, it is prudent to look into possible ways of shifting the plasmonic activity of transition (poor plasmonic) metals (*e.g.* rhodium,[19] vanadium,[20] platinum,[20] and ruthenium[21]) to the red so that efficient interaction with sunlight will be

[a] *Centre of New Technologies, University of Warsaw, Banacha 2c, 02-097 Warsaw, Poland. E-mail: tomasz.antosiewicz@uw.edu.pl*
[b] *Department of Applied Physics and Gothenburg Physics Centre, Chalmers University of Technology, 412-96 Göteborg, Sweden.*

RSC Advances Accepted Manuscript

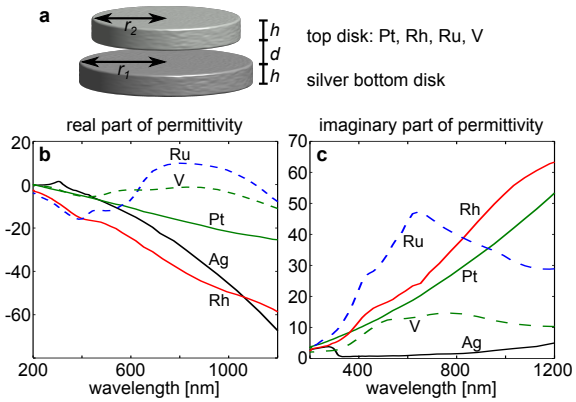

Fig. 1 a Two coupled metallic disks are used to investigate resonant energy transfer and absorption enhancement in one of the resonators. The bottom disk is made from a good plasmonic metal, silver, to couple efficiently light into localized plasmons and enhance absorption in the top disk made from poor plasmonic metals: Pt, Rh, Ru, and V. The radii of the disks are r_1 and r_2 for the bottom and top disks, respectively, their thickness is h and separation d. **b** Real and **c** imaginary parts of permittivity of the metals.[22] Notice the large variation of permittivities and a very low imaginary part of silver in comparison to other listed metals

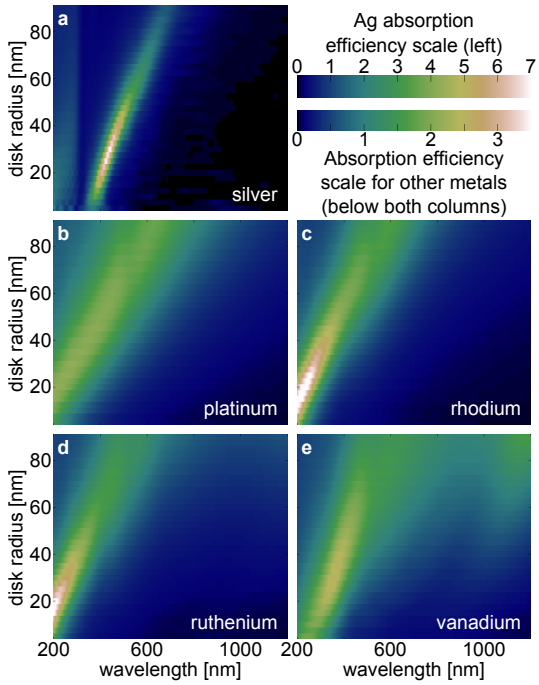

Fig. 2 Comparison of absorption efficiencies (absorption cross section to geometrical cross section) of **a** silver, **b** platinum, **c** rhodium, **d** ruthenium, and **e** vanadium disks. Silver, a good plasmonic metal, is characterised by a well defined narrow resonance (absorption efficiency up to 7), while the other metals exhibit much broader absorption peaks (absorption efficiency less than 3.5). With the exception of V, the poor plasmonic metals have spectra which are for equal disk radii blueshifted with respect to the Ag resonance, especially for Pt, Rh, and Ru. For $r_2 < 20$ nm these resonances are well below 300 nm, meaning that their interaction regime is outside the solar maximum

possible. A simple way is to use high-index substrates, yet this approach has limitations related to the available refractive indices. Another approach, the one investigated in this work, is to couple plasmonic resonances of adjacent nanoparticles and make use of the new hybridized resonances. We should note, that the complexity of any photocatalytic process, which includes light absorption, electron-hole separation and surface oxidation-reduction reactions, means that a simple enhancement of one of the steps may not translate into improved catalysis. However, if (plasmon-assisted) light absorption is the limiting step, we expect that enhancing it will improve the overall efficiency, assuming all other factors remain unchanged. Furthermore, the presented approach can be viewed not only as absorption enhancement, but also as shifting the optical activity of nanoparticles from one part of the spectrum into another.

Coupled plasmonic structure

Investigation of the variability and limits of absorption enhancement in heterometallic coupled resonators is best performed on a well-studied system, which is the reason behind using a plasmonic nanosandwich placed in vacuum,[23–28] as depicted in Fig. 1a. The efficiency of light-matter interactions of an object may be characterised by the quality factor (*e.g.* position-to-linewidth ratio $\omega/\Delta\omega$) of the resonances of its constituent elements. Here, one disk is assumed to be made of a good plasmonic metal, Ag, as it has a sharp response in the visible and its interband absorption occurs at wavelengths below 300 nm. Its radius r_1 is varied between 50 and 80 nm to be able to scan the LSPR across the peak of the solar spectrum. The second disk (radius r_2) is composed of various poor plasmonic metals, *i.e.* Pt, Rh, Ru, and V, where their permittivities are taken from literature.[22] Both disks have the same thickness $h = 20$ nm and the second one has a variable radius from 10 nm to r_1. They are separated by $d = 0$, 10, and 20 nm. Calculations are done using the finite-difference time-domain method with total-field/scattered-field excitation and absorbing boundary conditions. We use a nonuniform mesh with a minimum step of 1 nm around the disks and 8 nm far away from them with a graded transition region. The time step is calculated from Courant's stability criterion. Figure 1b,c presents the real and imaginary parts of permittivity of the metals used herein.

In order to quantify absorption tunability of plasmonic dimers it is first necessary to calculate the absorption baseline of its constituent elements. In Fig. 2 we plot the absorption

RSC Advances Accepted Manuscript

This journal is © The Royal Society of Chemistry [year]

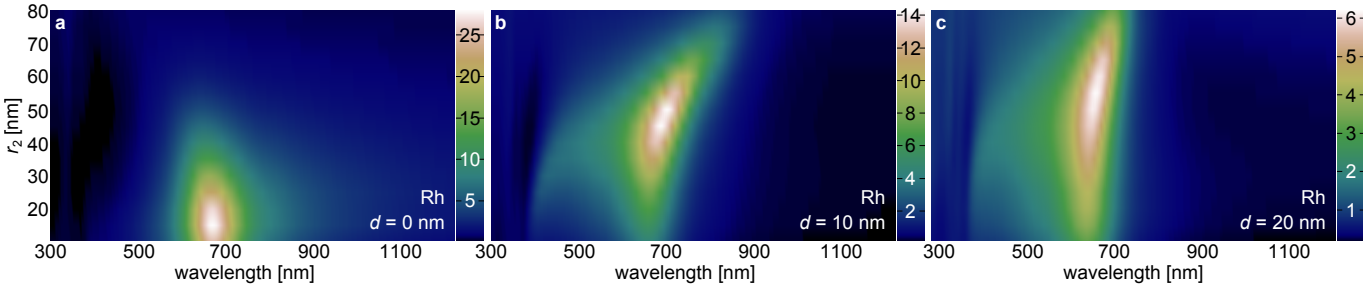

Fig. 3 Examples of wavelength-dependent absorption enhancement for rhodium on top of a silver disk of radius $r_1 = 80$ nm and resonator separations: **a** $d = 0$ nm, **b** $d = 10$ nm, and **c** $d = 20$ nm. The maximum enhancement follows the LSPR of the silver disk and within the range of investigated separations moves to larger r_2 values for increasing d. For other metals the qualitative spectral dependence is similar, however, quantitatively enhancement is lower and depends on the metal used. When r_1 is reduced the LSPR of the Ag disk blueshifts and, consequently, so does the enhancement peak

efficiency (absorption cross section normalized to geometrical cross section) of disks illuminated normally. The absorption spectrum of silver (Fig. 2a) is characterised by a sharp LSPR up to an amplitude of 7 that redshifts from *ca.* 400 to 700 nm, while at shorter wavelengths interband absorption manifests itself. In comparison to silver, the other metals have weaker – up to 2 for Pt, 2.5 for V, and 3.5 for both Rh and Ru – and broader resonances – between 2 and 4 times. However, their most important characteristic is that their spectra are shifted to the blue with respect to silver. This is indeed a signature of many poor plasmonic metals as was demonstrated recently.[29,30] Of the metals considered here disks 10 nm in radius have their resonances at or slightly below 200 nm with only vanadium exhibiting it at *ca.* 300 nm. The spectral location of their resonance is connected directly to the real parts of their permittivities. Let us recall that in the quasistatic case a sphere in vacuum exhibits a resonance when its permittivity $\varepsilon = -2$. Note, that $\varepsilon_{\mathrm{Ru}}$ and $\varepsilon_{\mathrm{Rh}}$ become -2 at ≈ 200 nm, coinciding with what is seen in Fig. 2c,d. Permittivities of Pt and V are redshifted with respect to Ru, hence their absorption spectra are not so far in the ultraviolet. The difference between Pt and V arises from losses, which are larger for Pt causing a slight blueshift.

Absorption characteristics of hetero-metallic plasmonic nanostructures

Interaction between resonators results in the appearance of two new, coupled modes. This mechanism is utilized here to enhance the optical response of the poor plasmonic (yet catalytic) metals and shift their LSPR into a spectral region of high intensity light (here we use solar illumination as an example). The wavelength resolved enhancement $E(\lambda) = \sigma_a^*(\lambda)/\sigma_a(\lambda)$, where σ_a^* and σ_a are wavelength dependent absorption cross sections of the catalytic metal disks in the structure and alone, respectively, is shown for three representative combinations of Rh as the top disk metal, $r_1 = 80$ nm, and varied d in Fig. 3.

In Figure 3a a rhodium disk is placed on top of a silver disk with $r_1 = 80$ nm. Maximum absorption enhancement occurs at *ca.* 650 nm for the smallest r_2 values and decreases as the Rh disk size increases. The case for small r_2 resembles that of a large optical antenna driving a smaller one at a frequency that is off the latter one's resonance. Hence, absorption enhancement is greatest at the wavelength at which the bottom silver disk (the large optical antenna) resonates. However, due to the two disks being in contact with one another, the efficiency decreases rapidly when r_2 increases and simultaneously experiences a blue shift. The system exhibits only one plasmon resonance supported by a metal which is neither Ag nor one of the poor plasmonic metals, but rather resembles a disk with material properties representative of a weighted sum. A single, yet heterogeneous metal disk is also the reason for the blue shift – when a plasmonic disk thickens, its resonance shifts to the blue. When the Rh disk is moved away from the silver resonator ($d = 10$ nm and 20 nm in Fig. 3b and c, respectively), the maximum enhancement decreases. The reason for this is a lowering of the coupling efficiency between the disks due to increased separation. Increased separation between the disks causes a red shift of the absorption enhancement (which follows the Ag resonance) as r_2 increases due to coupling between the disks and the resulting anticrossing of the two hybridized modes. For decreasing r_1 the Ag LSPR and the absorption enhancement blueshift, yet these observations hold.

Figure 4 presents total absorption enhancement in Rh, defined as

$$E_t = \frac{\int \sigma_a^*(\lambda) s(\lambda) d\lambda}{\int \sigma_a(\lambda) s(\lambda) d\lambda}, \qquad (1)$$

where $s(\lambda)$ is a weighing function of a light source (*e.g.* in our case the AM1.5 solar spectrum). The results are arranged into three branches with d as the defining criterion – $d = 0$ nm is

RSC Advances Accepted Manuscript

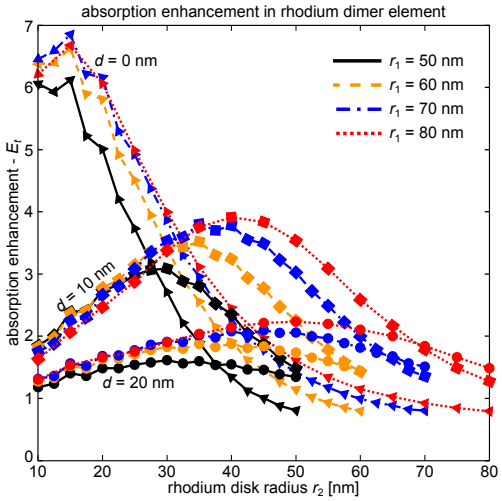

Fig. 4 Wavelength-integrated absorption enhancement [Eq. (1)] in rhodium dimer element due to coupling to the silver dimer element for different separations d and Ag disk radii r_1 as a function of the Rh disk radius r_2. Solid lines mark $r_1 = 50$ nm, dashed – 60 nm, dash-dotted – 70 nm, and dotted – 80 nm; symbols indicated separation of 0, 10, and 20 nm for triangles, diamonds, and circles, respectively. At $d = 0$ nm enhancement saturates at 7 for small Rh disks and decreases with increasing r_2. When the Rh disk moves away from the Ag one maximum enhancement decreases, but its maximum shifts toward larger radii

marked with triangles, $d = 10$ nm with squares, and $d = 20$ nm with circles. Maximum E_t is for touching disks and as d increases the overall enhancement also decreases. The observations made for the individual absorption spectra in Fig. 3 remain valid and explain the dependence seen in Fig. 4. Interestingly, maximum enhancements E_t for $d = 0$ nm are at least 6 for $r_2 < 20$ nm, irrespective of the Ag radius, and then decay as r_2 increases. For a separation of 10 nm the shape of E_t changes into a quasi-parabola with its maximum at $r_2 \approx r_1/2$ and a peak value increasing linearly with r_1. A similar r_2 dependence is observed for $d = 20$ nm, although in this case the maximum occurs at larger r_2 in comparison to the previous case.

In Fig. 5 we show the absorption enhancement for all considered poor plasmonic metals only for $d = 0$ nm for the smallest and the largest used Ag disk, because the enhancement for larger separations ($d > 0$ nm) is smaller than for $d = 0$ nm. Out of the four metals the largest enhancement, Ru is the metal which exhibits the largest absorption enhancement by a considerable margin – 9-fold enhancement for $r_1 = 50$ nm (E_t over the next best material – Rh – is almost 50% larger) and 13-fold for $r_1 = 80$ nm (twice better than Rh) for disks on the order of 20–30 nm in diameter. This advantage is also observed for other r_1 values. Rh, Pt, and V show weaker, but stable enhancements that are qualitatively similar and equal,

Table 1 Maximum light absorption enhancement in transition metal disks for $d = 0$ nm as function of silver disk radius.

	transition metal			
r_1	Pt	Rh	Ru	V
50 nm	5	6	9	4
60 nm	5.5	6.5	10.5	4.5
70 nm	5.5	7	12	4.5
80 nm	5.5	7	13	4.5

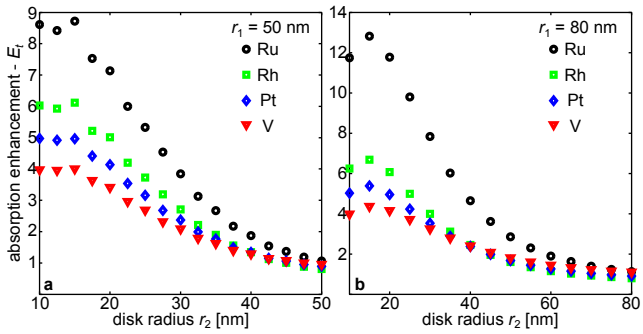

Fig. 5 Wavelength-integrated absorption enhancement [Eq. (1)] for touching dimer disks ($d = 0$ nm) as function of the top disk radius r_2 for **a** a silver resonator with $r_1 = 50$ nm and **b** 80 nm. Despite a large variation in permittivities (up to one order of magnitude) the absorption enhancement of the various metals is relatively similar. Despite an increase of the size of the Ag nanoantenna absorption enhancement in Rh, Pt, and V remains almost unchanged and only shows an increase in Ru

at maximum, 6, 5, and 4, respectively. Table 1 summarizes all maximum enhancements.

Discussion

The variability of observed absorption enhancements stems from the material response of the catalytic metal disks and is modified by the relative position (λ_0) of the coupled LSPR of the Ag resonator with respect to the spectral dependence of the weighing function $s(\lambda)$. Neglecting any low energy cut-offs (introduced by activation energies, *e.g.* Schottky barrier in a semiconductor or the energy level of an empty orbital of an adsorbed molecule), the spectral overlap of the absorption enhancement and $s(\lambda)$ is a key factor in determining how much energy in total can be captured by a catalytic metal nanoparticle. The absorption enhancement peak is asymmetric and for $\lambda < \lambda_0$ the decay is gradual in contrast to when $\lambda > \lambda_0$ (*cf.* Fig. 3). This implies, that coinciding the LSPR peak λ_0 with the peak of the weighing function (light spectrum) is not optimum, because the long wavelength part of the spectrum will not be used efficiently. In practice any given process imposes a minimum energy criterion. Hence, the nanostructure should

RSC Advances Accepted Manuscript

This journal is © The Royal Society of Chemistry [year]

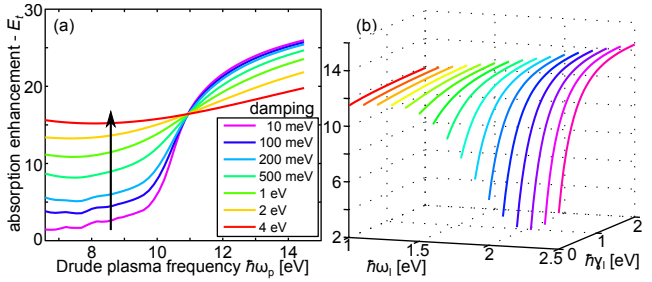

Fig. 6 Wavelength-integrated absorption enhancement [Eq. (1)] under solar illumination in a poor plasmonic metal disk coupled to a silver disk modelled as a Drude material with $\hbar\omega_{\mathrm{Ag}} = 9$ eV and $\hbar\gamma_{\mathrm{Ag}} = 65$ meV, and background permittivity 3.7 (LSPR at 2.1 eV). **a** The poor plasmonic metal is modelled as a Drude metal (ω_p, γ_p). For low damping absorption enhancement increases (nonlinearly) with ω_p; it is largest when the poor plasmonic metal disk's resonance blueshifts out of the solar maximum. Large damping smoothes out the enhancement. **b** Drude-Lorentz permittivity of the poor plasmonic disk with $\hbar\omega_p = 11$ eV and $\hbar\gamma_p = 0.5$ eV and variable Lorentz resonance frequency ω_l and line width γ_l. Absorption enhancement is almost constant when the Lorentz pole is far away from the LSPR. When the pole is close in frequency to the LSPR, small γ_l causes E_t to be low, while for large γ_l E_t is large

be made such that λ_0 is somewhat smaller than the wavelength corresponding to the cut-off energy (assuming that electrons excited to energies above the cut-off are used even if they do not match the empty state, *i.e.* their energy can thermalize until it matches that of the empty state). In the case of Ru with $r_1 = 80$ nm and $d = 20$ nm (Fig. 3c), the absorption enhancement is practically the same when considering any integration range between 280–800 and 280–1200 nm, signifying that such a structure under solar illumination is best used with a cut-off at approximately 1.5 eV.

Another factor determining absorption enhancement is the metal permittivity, whose influence we investigate using Drude and Drude-Lorentz materials. Despite this simplification, it is possible to identify qualitative dependencies which are useful in discussing real metals. This analysis is conducted using the coupled dipole approximation for one disk made from a low loss Drude metal and the second disk made of a poor plasmonic metal. In Fig. 6a we use Drude dispersion for the poor metal disk (plasma frequency $\hbar\omega_p$ from 6.5 to 14.5 eV, damping $\hbar\gamma_p$ from 10 meV to 4 eV). A large ω_p shifts the poor plasmonic metal disk's resonance out of the solar spectrum, decreasing its absorption in the optical regime. Coupling it to a good resonator attuned to the solar maximum increases absorption by more than an order of magnitude. For low damping absorption enhancement $E_t \approx 1$ when ω_p is small, but increases sharply for increasing plasma frequency. When γ_p increases, the resonance smears out and E_t becomes relatively insensitive to the plasma frequency.

The second plot, Fig. 6b, shows absorption enhancement when a Lorentz term (resonance position ω_l, damping γ_l) is added to the dispersion relation of the poor plasmonic metal. In this case absorption enhancement depends mostly on the overlap between the silver disk's LSPR (at 2.1 eV) and the Lorentz contribution to permittivity. When they are spectrally separated, E_t is insensitive to γ_l. When they overlap, E_t for a narrow Lorentzian is small, because initial absorption of an uncoupled poor plasmonic disk is already large. On the other hand, when γ_l is large only a negligible part of the Lorentzian overlaps with the LSPR and the potential for increase is large.

These observations help elucidate the variations in absorption enhancement calculated for real metals. Out of Pt and Rh, which exhibit a relatively smooth permittivity, larger E_t is observed in Rh, which has a larger plasma frequency and slightly larger $\mathrm{Im}(\varepsilon)$ than Pt. A comparison between Ru and V, both metals with very strong and discrete interband transitions in the visible, shows that Ru, having a larger γ_p and stronger Lorentzians of the two metals, is the metal which is characterized by a larger E_t.

Increased absorption in catalytic metals comes from coupling energy into them from incident light via the LSPR of the silver disk. One factor affecting this process is coupling of energy into the silver nanoantenna, this being quantified by the extinction efficiency which exhibits a maximum for a given radius. This energy should then be coupled into the adjacent catalytic nanoparticles with the distance between the two elements being another factor. The larger d is, the less efficient is the coupling and the peak absorption enhancement decreases with d.

The largest enhancements are observed for the smallest nanoparticles, which are on the order of $(20\,\mathrm{nm})^3$. It is expected, that smaller nanoparticles will exhibit even larger enhancements. They are not considered in this work, as size quantization and surface scattering would have to be included, as well possible changes to other scattering pathways.[31,32] Both, important for nanoparticles smaller than *ca.* 5 nm, induce red- or blueshifts of the LSPR, however, the expected magnitude of the shifts is on the order of a few hundred meV and this will not affect the expected enhancements significantly.[33] Surface scattering, on the other hand, will also contribute significantly to an increased width of the LSPR at sizes comparable to 20 nm, potentially affecting the results for (only) the smallest nanoparticles considered here. This effect has been previously included in the bulk damping and will increase it.[34] This particular contribution is expected to increase the absorption enhancement, as discussed in connection to Fig. 6a.

Finally, we would like to address the question of what is the ratio of energy deposited in the transition metal element to that of the whole nanostructure. Like the enhancement, it depends on all parameters considered here. and for small disks in on

RSC Advances Accepted Manuscript

the order of 0.05 to 0.1, while for big particles approaches 0.9. The low fraction of energy dissipated in the smallest nanoparticles (which have the largest enhancement) may seem to negate the approach, however, one has to remember that it is possible to place more small particles near the Ag resonator. In this manner the enhancement efficiency will not be changed significantly, but the total fraction of energy deposited in the increased number of transition metal nanoparticles will also increase.

Enhanced absorption in light of sum rules

Interaction of light with matter takes either of two routes – a photon is absorbed or scattered, elastically or inelastically – and results in removal of energy from an incident beam, *i.e.* extinction. The subject of extinction and its relation to the properties of matter has been a topic of many investigations, *e.g* the work of Purcell, who expressed the spectral integral of extinction in terms of the particle volume and static dielectric function,[35] or that of Sievers, who related it to the effective number of electrons in the scatterer.[36] While these so-called sum rules stem from causality consideration rather than first principles derivations,[37] the key result of such investigations is that extinction of an arbitrary structure, when integrated over the entire frequency range, is proportional to the volume of the object in question. This implies that the exact shape of the investigated particle is not important. Here we are interested in absorption, so while the above mentioned general rules cannot be applied strictly to our case, they provide important guidelines. One should observe that while absorption dominates for small particles (hence $\sigma_{\text{ext}} \approx \sigma_{\text{abs}}$), the exact boundary depends, among other things, on the refractive index of the surrounding medium and electromagnetic coupling may, under certain conditions, alter significantly the absorption-to-scattering branching ratio.[38,39]

We shall explore this issue by first considering one dipole in an external electric field E_0. Using the Kramers-Kronig properties of the polarizability as a retarded response function and general high-frequency properties of the polarizability, it is possible to show that the total integrated extinction cross section is equal to the instantaneous response of the dipole $\int \sigma_{\text{ext}}\,\mathrm{d}\omega = \pi V \omega_p^2/(2c) \propto N$. The preceding is nothing but the f-sum rule, with V being the volume occupied by the dipole of the system, ω_p the plasma frequency, c is the speed of light, and N the total number of electrons in V.

We now perform the same analysis for an interacting system of two dipoles coupled to E_0 and each other,[2] and focus on one of the dipoles. Since the polarizability vanishes for high frequencies at least as $1/\omega^2$, the coupling dependence in the dipole-dipole interaction term drops out of the integration. Thus the interacting dipole result is the same as for the non-interacting dipole result. Hence, total extinction for every part of a heterometalic nanostructure is constant. Fortunately there are two relaxing conditions in our case: we are only interested in total absorption and, more importantly, only in a predefined frequency region. The first point indicates that we can at the expense of scattering increase absorption. The second implies that, while any increase in one part of the spectrum is balanced by a proportional decrease in another part, appropriate engineering of the nanostructure assures that in the region of interest absorption is only increased and the corresponding decrease occurs outside of it. Hence, expressing our problem in terms of the equation in the preceding paragraph, we set cut-offs on the integration and for carefully chosen limits (frequency range) absorption may be increased considerably despite the fact that the number of electrons does not increase.

This approach is motivated by the fact that tailoring light-matter interactions for virtually any type of solar harvesting application introduces an inherent cut-off in energy that dictates that photons of lower energy will be lost; simultaneously the energy density of the solar spectrum below 300 nm is negligible. These two values, one of which depends on the considered problem (reaction), limit the range of usable energies in solar harvesting applications and the sum rules are no longer strictly valid. Importantly, some metal nanoparticles (especially for plasmon-assisted photocatalysis), depending on their size and the refractive index of the environment, will have their LSPRs in the UV[30] where the solar flux is small or nonexistent. Thus, shifting their resonances into the visible is beneficial. It is important to remember, however, that such shifting schemes are not limited to just the solar spectrum but, in fact, can be employed for any given photon source that is mismatched with respect to the LSPR resonance of the catalytic nanoparticles.

Summary and conclusions

The LSPR of nanoparticles made of catalytic metals is usually considerably weaker than that of coinage metals and for plasmon-assisted catalysis to be efficient an increase of the strength of the LSPR is beneficial. This is especially relevant for solar-driven photocatalysis on nanoparticles with diameters smaller than 10–20 nm, which have relatively large surface areas, as their LSPR occurs predominantly in the UV, well away from the solar maximum. In this work it was demonstrated, that by coupling catalytic metal nanoparticles with low-loss metal nanoantennas it is possible to increase the optical absorption in the nanoparticles by more than an order of magnitude. Enhanced absorption is conditioned by an enhanced LSPR and thus any physical processes that are mediated by the plasmon absorption channel are expected to be similarly amplified. While this was demonstrated for four arbitrarily chosen transition metals with catalytic properties, it is expected that other metals with similar (general) chemical and

RSC Advances Accepted Manuscript

This journal is © The Royal Society of Chemistry [year]

optical properties will behave in a very similar manner, *e.g.* bismuth,[40], nickel,[41] or palladium.[42] It was also shown how the material properties, permittivity, of poor metals affect the achievable absorption enhancement. Thus, similar coupling schemes may be employed in plasmon-enhanced chemical reactions (photocatalysis) that occur at the surfaces of metals with a weak plasmonic response.

The range of possible absorption enhancements was investigated for a variety of geometrical parameters of the heterometallic nanostructure. By choosing an appropriate size of the low-loss nanoantenna the enhancement spectrum of a catalytic metal nanoparticle can be made to overlap with photon energies that are larger than the activation energy of a given process. Such an approach makes optimum use of the illumination source. While the examples here were based on sunlight and employed shifting plasmonic activity from the UV to the visible, in principle it is possible to apply this coupling method to other light sources and match the enhancement profile to their spectrum. This matching would allow for efficient usage of light in plasmon-assisted photocatalysis with an additional benefit of that photocatalysis at surfaces may be more flexible at controlling single elementary step energetics than thermal catalysis.[13,21]

Finally, it is important to note that photocatalysis is a complicated process involving not only light absorption, but also such steps like electron-hole separation and surface oxidation-reduction reactions and can be limited by any number of effects like recombination or mass transfer. Thus, simply increasing the rate of energy absorption by some factor may not lead to a corresponding increase of the photocatalytic rate. However, if a given photocatalytic system is not constricted by any limits except for light absorption, then all else equal, we expect that increased absorption should translate into greater photocatalytic efficiencies.

Acknowledgements

Support for this work was provided by the Foundation for Polish Science via the project HOMING PLUS/2013-7/1 and the Swedish Foundation for Strategic Research.

References

1 H. Chalabi, D. Schoen and M. L. Brongersma, *Nano Lett.*, 2014, **14**, 1374–1380.
2 T. J. Antosiewicz, S. P. Apell, V. Claudio and M. Käll, *Opt. Express*, 2012, **20**, 524–533.
3 M. Yilmaz, E. Senlik, E. Biskin, M. S. Yavuz, U. Tamer and G. Demirel, *Phys. Chem. Chem. Phys.*, 2014, **16**, 5563–5570.
4 M. Abdulla-Al-Mamun, Y. Kusumoto, T. Zannat and M. S. Islam, *Phys. Chem. Chem. Phys.*, 2011, **13**, 21026–21034.
5 W. M. Saj, T. J. Antosiewicz, J. Pniewski and T. Szoplik, *Opto-Electron. Rev.*, 2006, **14**, 243–251.
6 A. Ahmadivand and S. Golmohammadi, *Opto-Electron. Rev.*, 2014, **22**, 101–108.
7 C. D. Bohn, A. Agrawal, Y. Lee, C. J. Choi, M. S. Davis, P. M. Haney, H. J. Lezec and V. A. Szalai, *Phys. Chem. Chem. Phys.*, 2014, **16**, 6084–6091.
8 P. Christopher, H. Xin and S. Linic, *Nature Chem.*, 2011, **3**, 467–472.
9 C. An, J. Wang, J. Liu, S. Wang and Q.-H. Zhang, *RSC Adv.*, 2014, **4**, 2409–2413.
10 S. Mukherjee, F. Libisch, N. Large, O. Neumann, L. V. Brown, J. Cheng, J. B. Lassiter, E. A. Carter, P. Nordlander and N. J. Halas, *Nano Lett.*, 2013, **13**, 240–247.
11 P. Wang, B. Huang, X. Qin, X. Zhang, Y. Dai, J. Wei and M.-H. Whangbo, *Angew. Chem., Int. Ed.*, 2008, **47**, 7931–7933.
12 S. Linic, P. Christopher, H. Xin and A. Marimuthu, *Acc. Chem. Res.*, 2013, **46**, 1890–1899.
13 M. J. Kale, T. Avanesian and P. Christopher, *ACS Catal.*, 2014, **4**, 116–128.
14 B. Hammer and J. K. Nørskov, *Nature*, 1995, **376**, 238–240.
15 P. Wang, B. Huang, Y. Dai and M.-H. Whangbo, *Phys. Chem. Chem. Phys.*, 2012, **14**, 9813–9825.
16 C. Clavero, *Nature Photon.*, 2014, **8**, 95–103.
17 M. I. Litter, *Appl. Catal. B*, 1999, **23**, 89–114.
18 D. Ghosh, S. Pradhan, W. Chen and S. Chen, *Chem. Mater.*, 2008, **20**, 1248–1250.
19 J.-L. Pellaegatta, C. Blandy, V. Colliére, R. Choukroun, B. Chaudret, P. Cheng and K. Philippot, *J. Mol. Catal. A*, 2002, **178**, 55–61.
20 M. Shen, H. Guo and F. Zaera, *Top. Catal.*, 2011, **54**, 482–489.
21 M. Bonn, S. Funk, C. Hess, D. N. Denzler, C. Stampfl, M. Scheffler, M. Wolf and G. Ertl, *Science*, 1999, **285**, 1042–1045.
22 *Handbook of Optical Constants of Solids*, ed. E. D. Palik, Academic Press: New York, 1985, 1991, 1997.
23 C. Helgert, C. Rockstuhl, C. Etrich, C. Menzel, E.-B. Kley, A. Tüennermann, F. Lederer and T. Pertsch, *Phys. Rev. B*, 2009, **79**, 233107.
24 C. Wadell, T. J. Antosiewicz and C. Langhammer, *Nano Lett.*, 2012, **12**, 4784–4790.
25 C. Helgert, C. Rockstuhl, C. Etrich, E.-B. Kley, A. Tüennermann, F. Lederer and T. Pertsch, *Appl. Phys. A*, 2011, **103**, 591–595.
26 T. J. Antosiewicz, S. P. Apell, C. Wadell and C. Langhammer, *J. Phys. Chem. C*, 2012, **116**, 20522–20529.
27 G. Armelles, A. Cebollada, A. García-Martín, M. U. González, F. García, D. Meneses-Rodríguez, N. de Sousa and L. S. Froufe-Pérez, *Opt. Express*, 2013, **21**, 27356–27370.
28 Z. Li, T. D. Dao, T. Nagao and M. Yoshino, *Microelectron. Eng.*, 2014, **127**, 34–39.
29 J. M. McMahon, G. C. Schatz and S. K. Gray, *Phys. Chem. Chem. Phys.*, 2013, **15**, 5415–5423.
30 J. M. Sanz, D. Ortiz, R. A. de la Osa, J. M. Saiz, F. González, A. S. Brown, M. Losurdo, H. O. Everitt and F. Moreno, *J. Phys. Chem. C*, 2013, **117**, 19606–19615.
31 Y. Fan, J. Li, H. Chen, X. Lu and X. Liu, *Opto-Electron. Rev.*, 2014, **22**, 36–40.
32 R. C. Monreal, S. P. Apell and T. J. Antosiewicz, *Opt. Express*, 2014, **22**, 24994–25004.
33 R. C. Monreal, T. J. Antosiewicz and S. P. Apell, *New J. Phys*, 2013, **15**, 083044.
34 K. Kolwas and A. Derkachova, *J. Quant. Spectrocs. Radiat. Transfer*, 2013, **114**, 45–55.
35 E. M. Purcell, *Astrophys. J.*, 1969, **158**, 433–440.
36 A. J. Sievers, *Opt. Commun.*, 1994, **109**, 71–74.
37 M. I. Mishchenko, *J. Opt. Soc. Am. A*, 2008, **25**, 2893–2895.
38 T. J. Antosiewicz, S. P. Apell, M. Zäch, I. Zorić and C. Langhammer, *Phys. Rev. Lett.*, 2012, **109**, 247401.

RSC Advances Accepted Manuscript

39 T. J. Antosiewicz and S. P. Apell, *Opt. Express*, 2014, **22**, 2031–2042.
40 Z. Wang, C. Jiang, R. Huang, H. Peng and X. Tang, *J. Phys. Chem. C*, 2014, **118**, 1155–1160.
41 J. Park, E. Kanf, S. U. Son, H. M. Park, M. K. Lee, J. Kim, K. W. Kim, H. Noh, J.-H. Park, C. J. Bae, J.-G. Park and T. Hyeon, *Adv. Mater.*, 2005, **17**, 429–434.
42 R. Li, P. Zhang, Y. Huang, C. Chen and Q. Chen, *ACS Appl. Mater. Interfaces*, 2013, **5**, 12695–12700.

RSC Advances Accepted Manuscript

This journal is © The Royal Society of Chemistry [year]